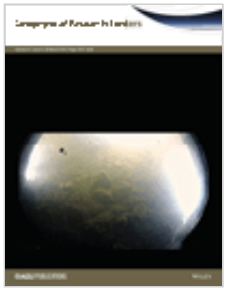

Volume 39, Issue 15

16 August 2012

Brief Detailed

Atmospheric Science

Gravity wave momentum flux spectra observed from satellite in the summertime subtropics: Implications for global modeling

M. Ern, P. Preusse

First Published: 15 August 2012 Vol: 39, L15810 | DOI: 10.1029/2012GL052659

KEY POINTS

- Gravity wave spectra are derived from satellite in the summertime subtropics
- Over deep convection the spectrum is enhanced at short horizontal wavelengths
- Momentum flux of convective gravity waves is important on zonal average

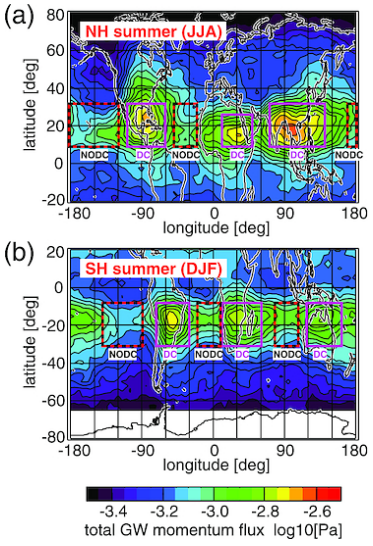

1 of 2

The role of shortwave radiation in the 2007 Arctic sea ice anomaly

Eric A. Nussbaumer, Rachel T. Pinker

First Published: 14 August 2012 Vol: 39, L15808 | DOI: 10.1029/2012GL052415

KEY POINTS

- Shortwave radiation not the driver of 2007 Arctic sea ice anomaly
- Importance of high quality information in addressing climate in the Arctic
- Cloud information is consistent with information on radiative fluxes

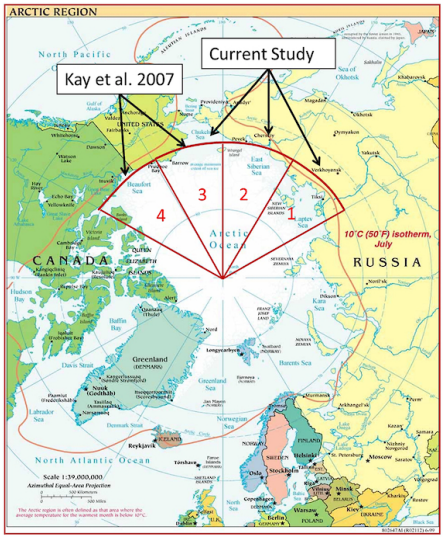

1 of 4

Where is the level of neutral buoyancy for deep convection?

Hanii Takahashi, Zhengzhao Luo

First Published: 14 August 2012 Vol: 39, L15809 | DOI: 10.1029/2012GL052638

KEY POINTS

- The classic definition of LNB is insufficient for describing deep convection
- CloudSat radar data can help determine the effective LNB
- Comparing the two yields insights into the underlying convective processes

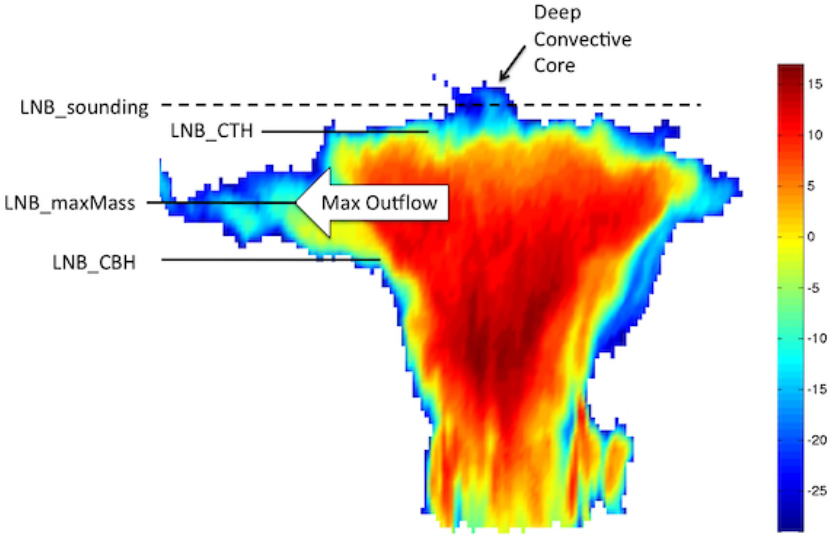

1 of 2

Lagrangian decomposition of the Hadley and Ferrel cells

J. Kjellsson, K. Döös

First Published: 11 August 2012 Vol: 39, L15807 | DOI: 10.1029/2012GL052420

KEY POINTS

- We visualize and quantify mass transports that cancel in the Eulerian mean
- Large re-circulation cancels near-isentropic transport in mid-latitudes
- We show and discuss how well the Eulerian mean represents Lagrangian transport

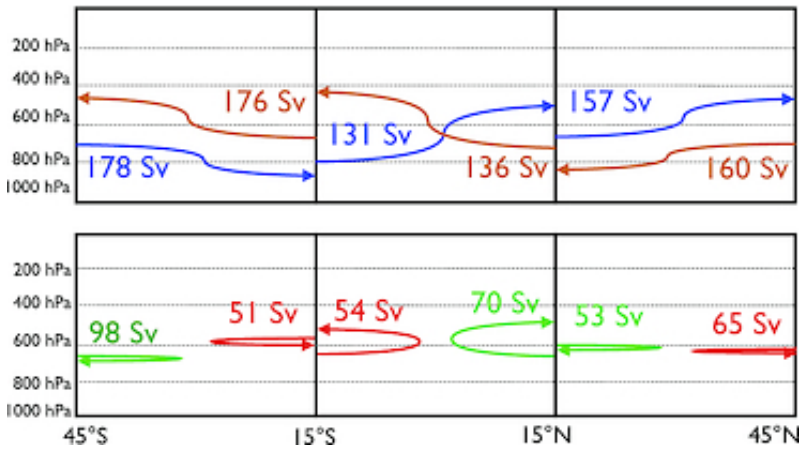

1 of 2

The effectiveness of N_2O in depleting stratospheric ozone

Laura E. Revell, Greg E. Bodeker, Dan Smale, Ralph Lehmann, Petra E. Huck, Bryce E. Williamson, Eugene Rozanov, Hamish Struthers

First Published: 9 August 2012 Vol: 39, L15806 | DOI: 10.1029/2012GL052143

KEY POINTS

- NOx-induced ozone destruction slows through the 21st century
- Due to chemical, radiative and dynamical changes in the stratosphere
- The effectiveness of N2O as an ODS is weakened by elevated CH4 concentrations

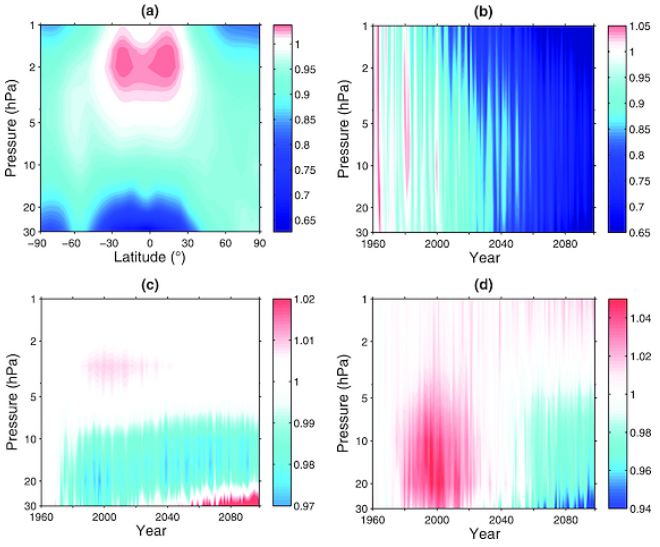

1 of 3

Simulated winter circulation types in the North Atlantic and European region for preindustrial and glacial conditions

D. Hofer, C. C. Raible, N. Merz, A. Dehnert, J. Kuhlemann

First Published: 7 August 2012 Vol: 39, L15805 | DOI: 10.1029/2012GL052296

KEY POINTS

- Preindustrial and glacial circulation types in the North Atlantic clearly differ
- The topography is the main reason for the differences
- Changes in the circulation types explain up to 60% of the precipitation changes

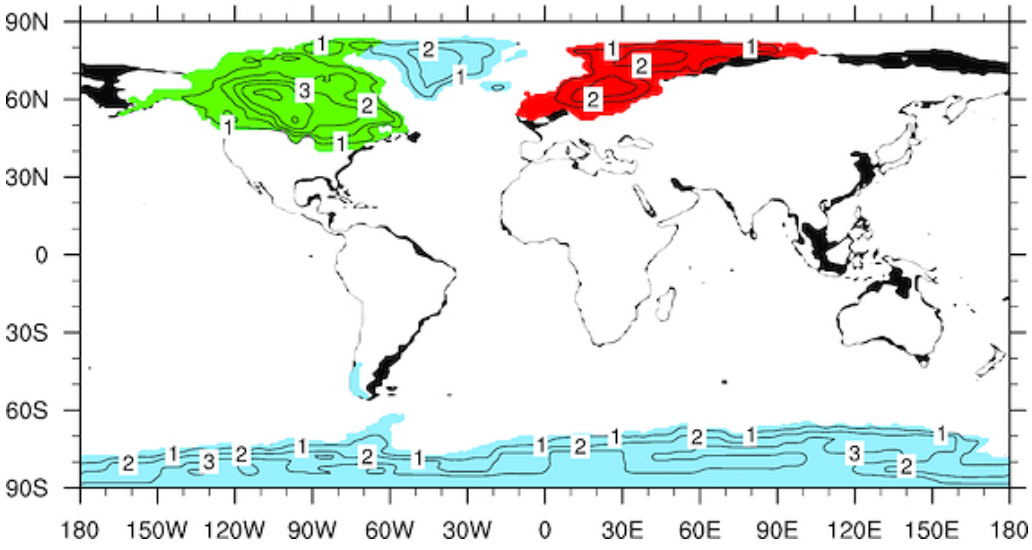

1 of 4

Increasing atmospheric burden of ethanol in the United States

J. A. de Gouw, J. B. Gilman, A. Borbon, C. Warneke, W. C. Kuster, P. D. Goldan, J. S. Holloway, J. Peischl, T. B. Ryerson, D. D. Parrish, et al

First Published: 4 August 2012 Vol: 39, L15803 | DOI: 10.1029/2012GL052109

KEY POINTS

- The use of fuel ethanol has increased by a factor of ten in the last decade
- Measurements show that ethanol in urban air has increased strongly
- Acetaldehyde, a hazardous air pollutant produced from ethanol, has decreased

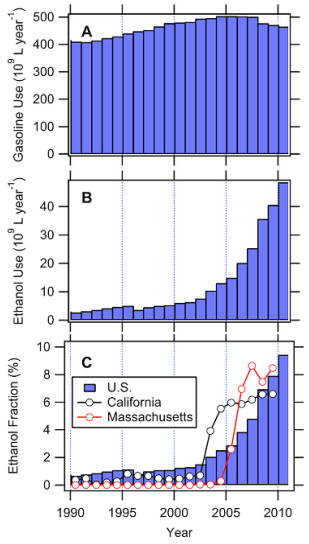

1 of 4

Scales of variability of black carbon plumes over the Pacific Ocean

N. M. Weigum, P. Stier, J. P. Schwarz, D. W. Fahey, J. R. Spackman

First Published: 4 August 2012 Vol: 39, L15804 | DOI: 10.1029/2012GL052127

KEY POINTS

- Black carbon plumes represent important features of total BC in the atmosphere
- BC plumes account for a large degree of total BC variability
- Most BC plumes occur on scales roughly half the size of climate models resolutions

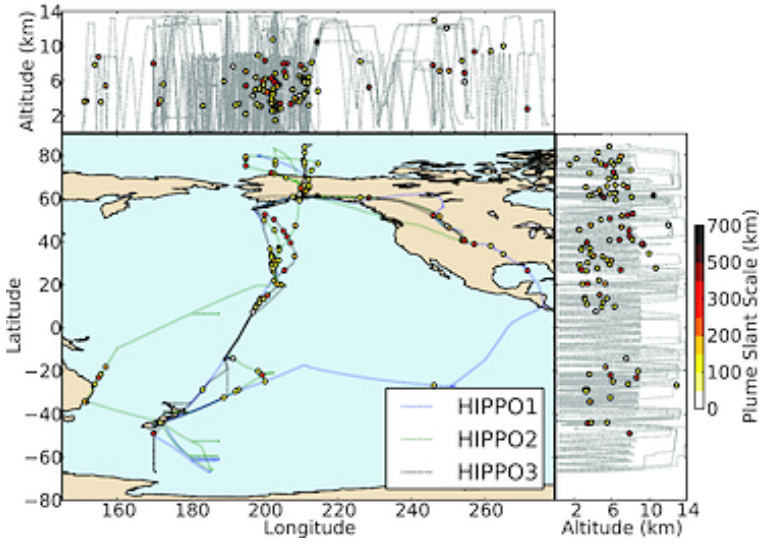

1 of 3

Weather and climate analyses using improved global water vapor observations

Thomas H. Vonder Haar, Janice L. Bytheway, John M. Forsythe

First Published: 3 August 2012 Vol: 39, L15802 | DOI: 10.1029/2012GL052094

KEY POINTS

- The NVAP-M dataset reprocesses and extends the existing NVAP dataset
- NVAP-M provides three product types to suit varying user needs
- Science applications include variability on various spatial/temporal scales

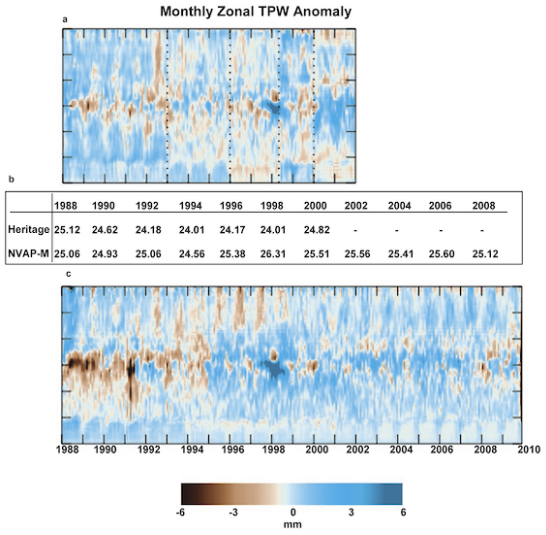

1 of 5

Double sodium layers observation over Beijing, China

Jihong Wang, Yong Yang, Xuewu Cheng, Guotao Yang, Shalei Song, Shunsheng Gong

First Published: 3 August 2012 Vol: 39, L15801 | DOI: 10.1029/2012GL052134

KEY POINTS

- Seventeen double sodium layer events were observed during 319 observation nights
- The basic features of the double sodium layer were described and analyzed
- The formation and disappearance of the double sodium layer were discussed

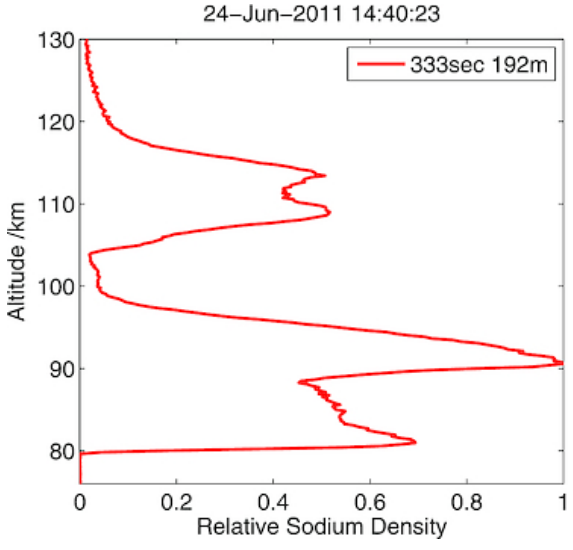

1 of 4

Climate

Constraining cloud lifetime effects of aerosols using A-Train satellite observations

Minghuai Wang, Steven Ghan, Xiaohong Liu, Tristan S. L'Ecuyer, Kai Zhang, Hugh Morrison, Mikhail Ovchinnikov, Richard Easter, Roger Marchand, Duli Chand, et al

First Published: 15 August 2012 Vol: 39, L15709 | DOI: 10.1029/2012GL052204

KEY POINTS

- A new metric is shown to be a good measure of cloud lifetime effects of aerosols
- Satellite-derived Spop is significantly lower than those from global models
- Satellite observations imply a substantially smaller aerosol indirect effect

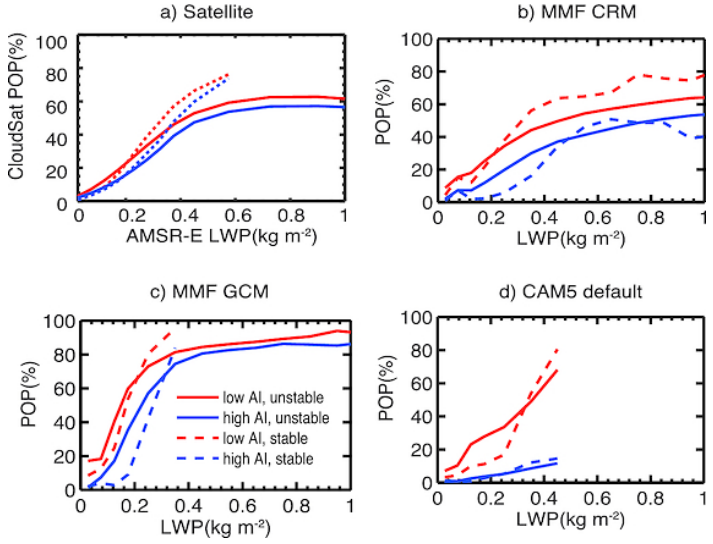

1 of 3

Nonlinear climate response to regional brightening of tropical marine stratocumulus

Spencer Hill, Yi Ming

First Published: 14 August 2012 Vol: 39, L15707 | DOI: 10.1029/2012GL052064

KEY POINTS

- Brightening clouds over SE subtropical Pacific induces La Nina-like response
- Nonlinear response to seeding different regions
- ~1/2 forcing by direct scattering; was neglected in prior response studies

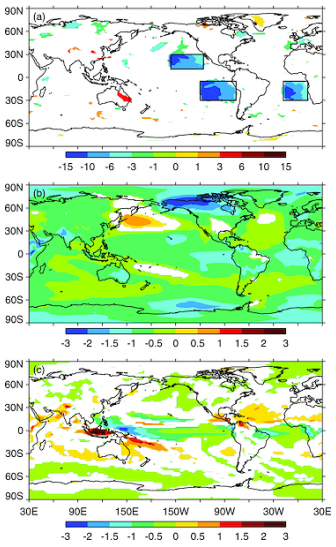

1 of 2

Tropical circulation and hydrological cycle response to orbital forcing

V. C. Khon, W. Park, M. Latif, I. I. Mokhov, B. Schneider

First Published: 14 August 2012 Vol: 39, L15708 | DOI: 10.1029/2012GL052482

KEY POINTS

- Intensification of the SH winter Hadley cell for the early Holocene and Eemian
- Walker circulation's rising branch is shifted westward towards the Indian Ocean
- WES feedback plays key role in intensification of the Hadley circulation

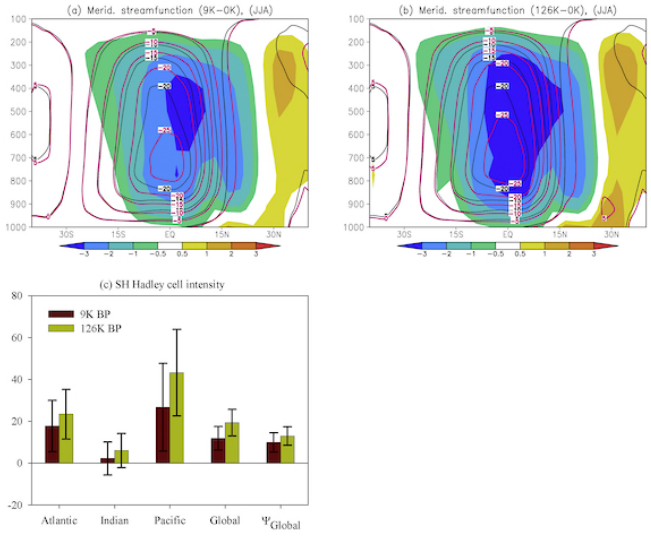

1 of 4

Cloud base and top heights in the Hawaiian region determined with satellite and ground-based measurements

Chunxi Zhang, Yuqing Wang, Axel Lauer, Kevin Hamilton, Feiqin Xie

First Published: 11 August 2012 Vol: 39, L15706 | DOI: 10.1029/2012GL052355

KEY POINTS

- The best estimate of cloud climatology in the Hawaiian region is given
- Different data sources provide quite consistent and robust results
- Results can be used to evaluate climate simulations

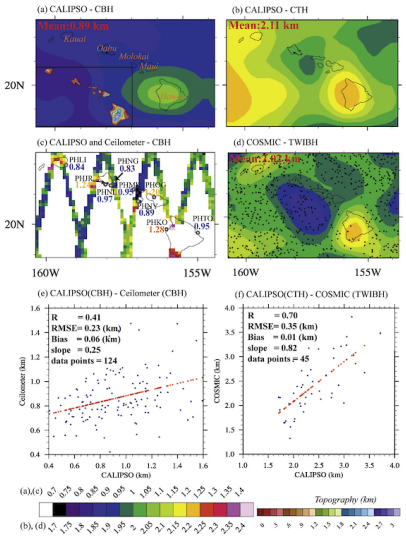

1 of 3

Elevated methane concentrations in trees of an upland forest

Kristofer R. Covey, Stephen A. Wood, Robert J. Warren II, Xuhui Lee, Mark A. Bradford

First Published: 9 August 2012 Vol: 39, L15705 | DOI: 10.1029/2012GL052361

KEY POINTS

- The production of methane inside trees is not limited to lowland soils
- Production rates vary seasonally, and with tree species
- Archea active in trees produce significant quantities of methane

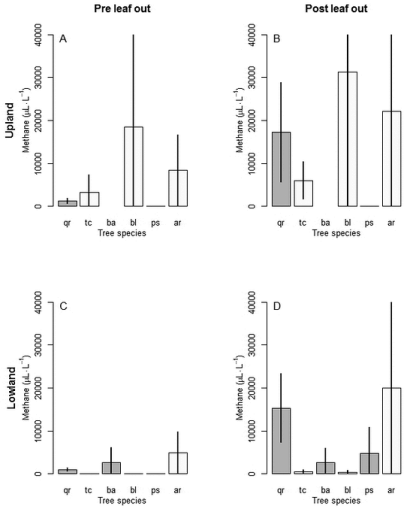

1 of 1

Field information links permafrost carbon to physical vulnerabilities of thawing

Jennifer W. Harden, Charles D. Koven, Chien-Lu Ping, Gustaf Hugelius, A. David McGuire, Phillip Camill, Torre Jorgenson, Peter Kuhry, Gary J. Michaelson, Jonathar A. O'Donnell, et al

First Published: 7 August 2012 Vol: 39, L15704 | DOI: 10.1029/2012GL051958

KEY POINTS

- Field-based knowledge of soil C and N data improves models of Arctic C and N
- Specific C and N vulerabilities of Arctic soils to thaw are identified
- International dataset is made available

Open Access Highlight

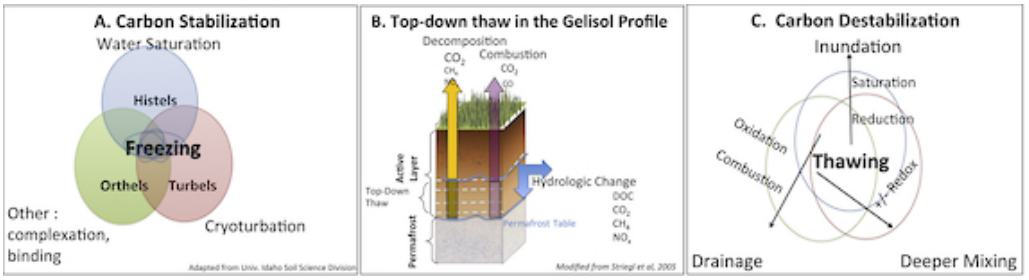

1 of 3

A global picture of the first abrupt climatic event occurring during the last glacial inception

E. Capron, A. Landais, J. Chappellaz, D. Buiron, H. Fischer, S. J. Johnsen, J. Jouzel, M. Leuenberger, V. Masson-Delmotte, T. F. Stocker

First Published: 4 August 2012 Vol: 39, L15703 | DOI: 10.1029/2012GL052656

KEY POINTS

- A 3 degree C abrupt warming ending the last interglacial in Greenland
- Potentially, a regional origin for the initiation of rapid climate variability
- Interplay between orbitally-driven glacial inception and abrupt climate change

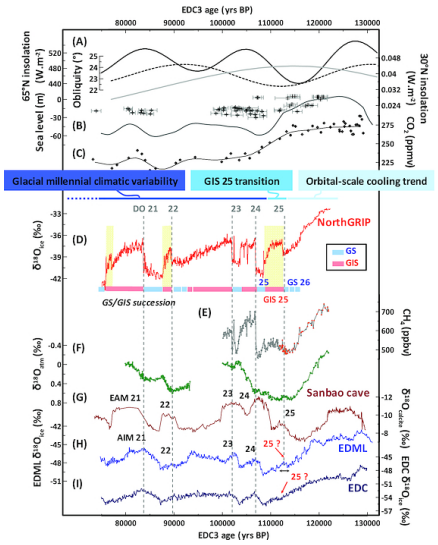

1 of 2

The changing impact of El Niño on US winter temperatures

Jin-Yi Yu, Yuhao Zou, Seon Tae Kim, Tong Lee

First Published: 2 August 2012 Vol: 39, L15702 | DOI: 10.1029/2012GL052483

KEY POINTS

- Different impacts of two type El Nino on US temperatures
- Difference in regions of the US that are most sensitive to each type of El Nino
- Different impacts are related with differing atmospheric wave train responses

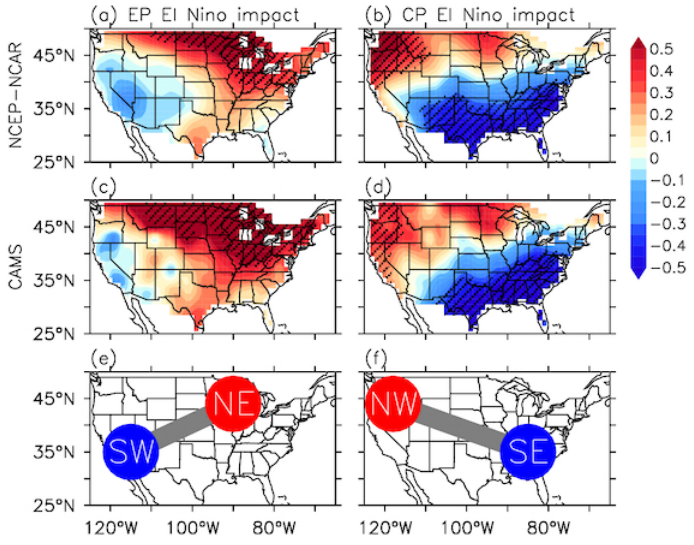

1 of 6

Hydrology and Land Surface Studies

A method to improve satellite soil moisture retrievals based on Fourier analysis

Jinyang Du

First Published: 14 August 2012 Vol: 39, L15404 | DOI: 10.1029/2012GL052435

KEY POINTS

- Fourier analysis based method improves soil moisture retrieval accuracy
- High-frequency component of the observations is sensitive to surface changes
- The high-frequency component is a new indicator to monitor surface soil moisture

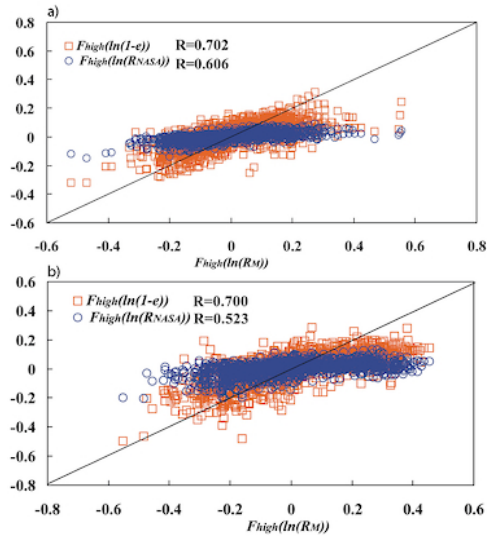

1 of 2

Too early to infer a global NPP decline since 2000

Anders Ahlström, Paul A. Miller, Benjamin Smith

First Published: 10 August 2012 Vol: 39, L15403 | DOI: 10.1029/2012GL052336

KEY POINTS

- Globally, NPP has increased from 2000 through 2009
- Climate- and satellite-based c-cycle modelling disagree on recent global trends
- Droughts are a major driver of NPP variations in the southern hemisphere

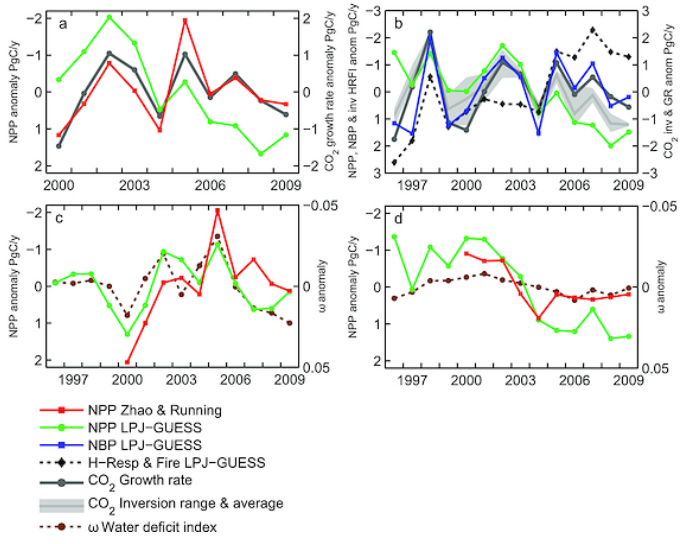

1 of 1

The planetary water drama: Dual task of feeding humanity and curbing climate change

J. Rockström, M. Falkenmark, M. Lannerstad, L. Karlberg

First Published: 1 August 2012 Vol: 39, L15401 | DOI: 10.1029/2012GL051688

KEY POINTS

- Food production and carbon sequestration compete for freshwater
- Water for food and carbon sequestration exceed planetary water constraints
- Projected biomass water consumption aggravates current regional water shortages

Highlight

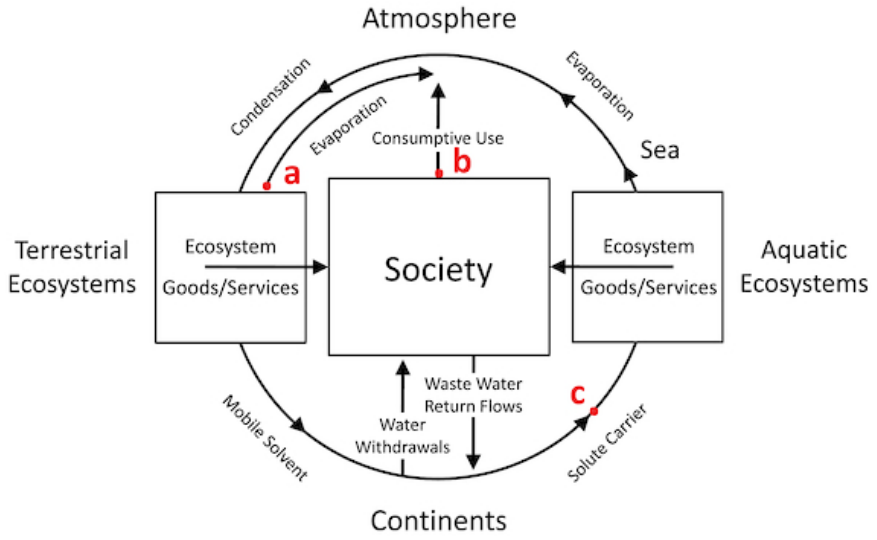

1 of 3

Morphometric dating of the fluvial landscape response to a tectonic perturbation

Alain Demoulin

First Published: 1 August 2012 Vol: 39, L15402 | DOI: 10.1029/2012GL052201

KEY POINTS

- Landscape metric R and derived SR index provide age estimate of uplift events
- SR index is in inverse power relation with time
- Response time of fluvial landscape to a tectonic perturbation is about 5 My

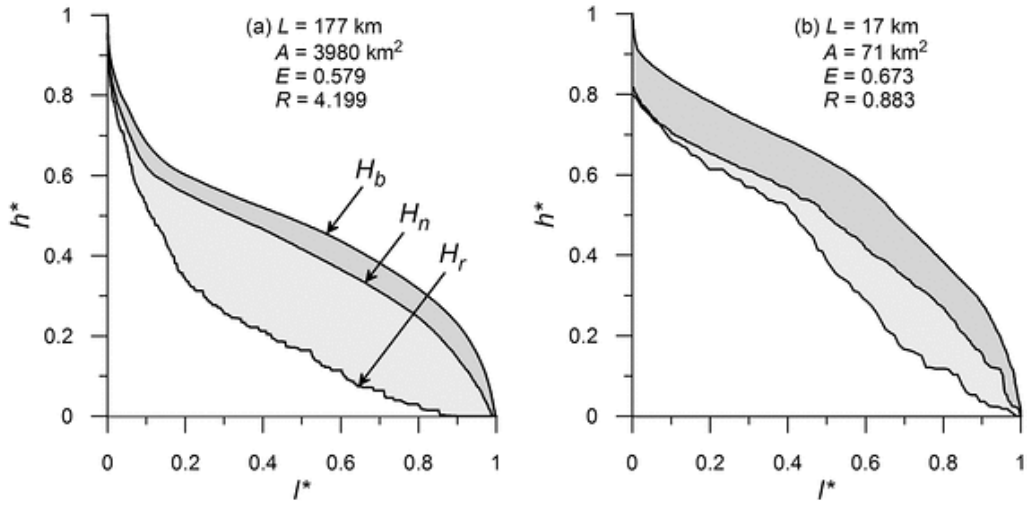

1 of 4

Process-based approach to CO_2 leakage detection by vadose zone gas monitoring at geologic CO_2 storage sites

K. D. Romanak, P. C. Bennett, Changbing Yang, Susan D. Hovorka

First Published: 15 August 2012 Vol: 39, L15405 | DOI: 10.1029/2012GL052426

KEY POINTS

- Gas relationships show carbon cycling processes
- Method is an innovative new way to distinguish CO2 leakage from depth
- The method has broad implications for geoscience

Highlight

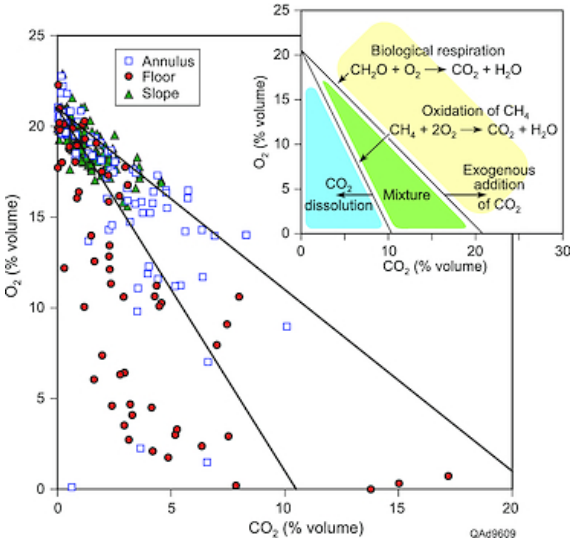

1 of 4

Oceans

Tectonic and climatic controls on long-term silicate weathering in Asia since 5 Ma

Shiming Wan, Peter D. Clift, Anchun Li, Zhaojie Yu, Tiegang Li, Dengke Hu
First Published: 15 August 2012 Vol: 39, L15611 | DOI: 10.1029/2012GL052377

KEY POINTS

- We reconstruct the history of silicate weathering in Asia since 5 Ma
- Our study shows a general decrease in chemical weathering intensity in Asia
- Our study further confirms Raymo's uplift-weathering hypothesis

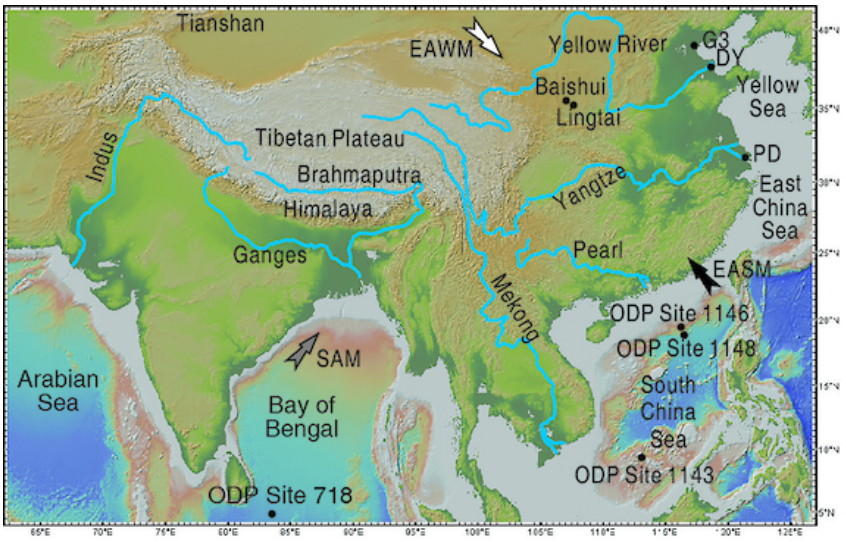

1 of 2

On the proportion of ballast versus non-ballast associated carbon export in the surface ocean

Frédéric A. C. Le Moigne, Richard J. Sanders, María Villa-Alfageme, Adrian P. Martin, Katsiaryna Pabortsava, Hélène Planquette, Paul J. Morris, Sandy J. Thomalla
First Published: 11 August 2012 Vol: 39, L15610 | DOI: 10.1029/2012GL052980

KEY POINTS

- Variability of CCs is linked to the PCS at sampling time
- Proportion of non-ballast associated sinking POC is 73% in the Southern Ocean
- Large non-ballast associated pool may explained low transfer efficiency

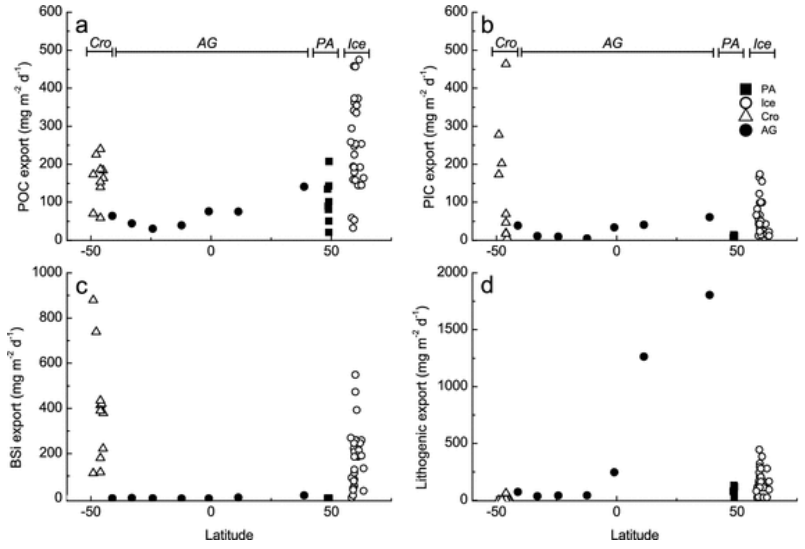

1 of 1

Revealing forerunners on Envisat's wave mode ASAR using the Global Seismic Network

R. Husson, F. Ardhuin, F. Collard, B. Chapron, A. Balanche

First Published: 10 August 2012 Vol: 39, L15609 | DOI: 10.1029/2012GL052334

KEY POINTS

- Seismic noise helps detect swell forerunners with SAR in open ocean
- Swell fields associated to their ocean-wide seismic noise signatures using SAR
- Storm source triangulation using swell forerunners signature in seismic noise

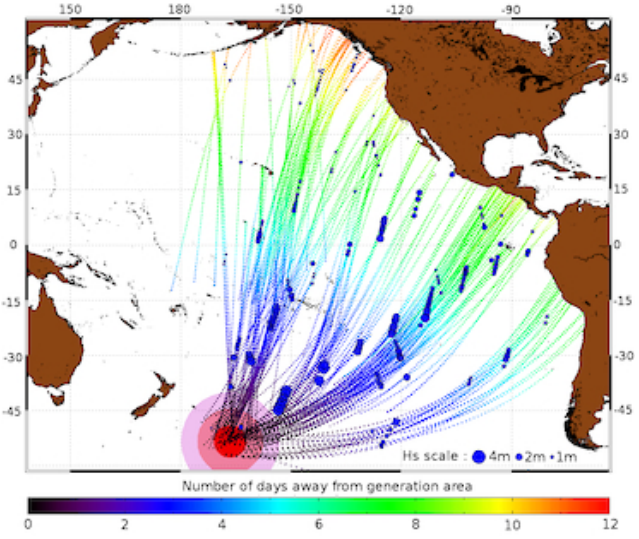

1 of 3

Oceanic transports through the Solomon Sea: The bend of the New Guinea Coastal Undercurrent

Florent Gasparin, Alexandre Ganachaud, Christophe Maes, Frédéric Marin, Gérard Eldin

First Published: 9 August 2012 Vol: 39, L15608 | DOI: 10.1029/2012GL052575

KEY POINTS

- Application of a geostrophic inverse box model to the Coral Sea
- Description of the horizontal and vertical structure of the current
- Discussion with water mass properties and heat transports

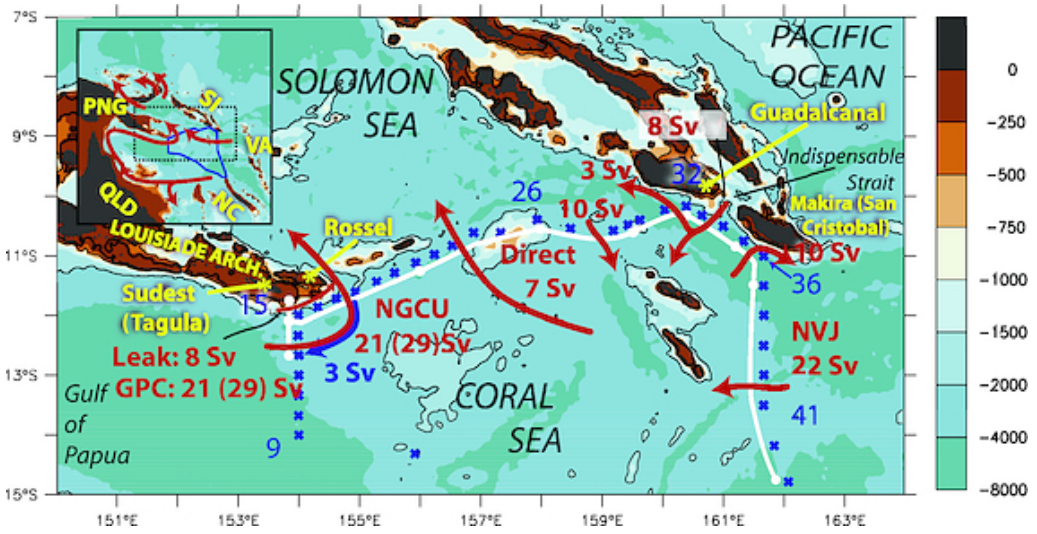

1 of 3

Satellite observations of an annual cycle in the Agulhas Current

M. Krug, J. Tournadre

First Published: 9 August 2012 Vol: 39, L15607 | DOI: 10.1029/2012GL052335

KEY POINTS

- There is an annual cycle in the Agulhas Current
- The annual cycle dominates the variability in the Agulhas Current
- A cross-stream approach is needed for Agulhas Current variability

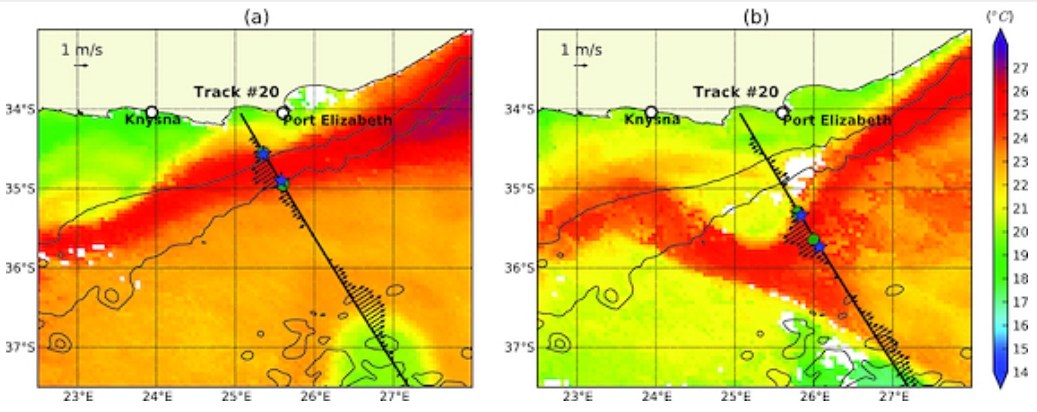

1 of 4

Correction to "North Pacific Gyre Oscillation modulates seasonal timing and ecosystem functioning in the California Current upwelling system"

F. Chenillat, P. Rivière, X. Capet, E. Di Lorenzo, B. Blanke

First Published: 8 August 2012 Vol: 39, L15606 | DOI: 10.1029/2012GL053111

Free

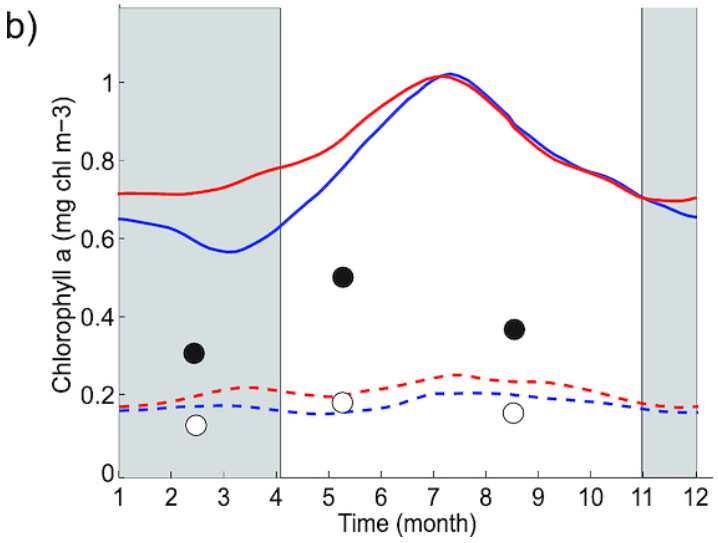

1 of 1

Could satellite altimetry have improved early detection and warning of the 2011 Tohoku tsunami?

B. D. Hamlington, R. R. Leben, O. A. Godin, E. Gica, V. V. Titov, B. J. Haines, S. D. Desai

First Published: 8 August 2012 Vol: 39, L15605 | DOI: 10.1029/2012GL052386

KEY POINTS

- NRT satellite altimetry measurements are used to detect the Tohoku tsunami
- Satellite altimetry can be used as a system for the NRT detection of tsunamis
- Satellite altimetry could improve tsunami predictions made by models

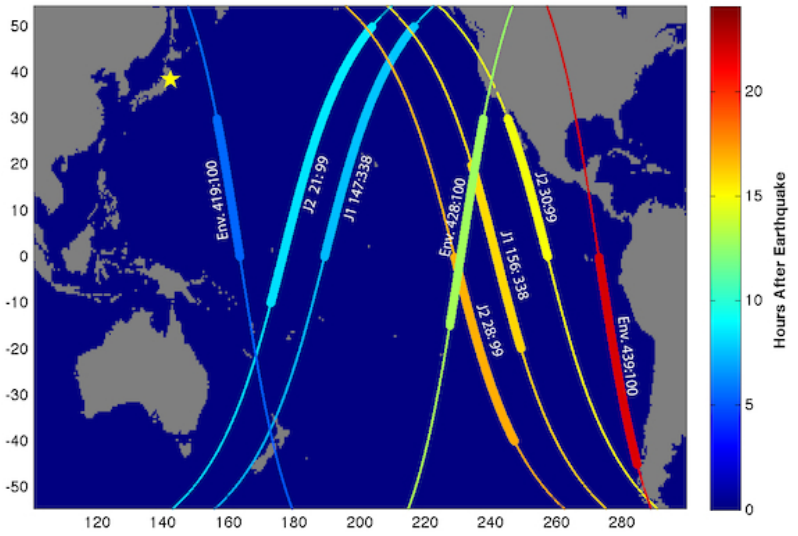

1 of 3

A dipole pattern of the sea surface height anomaly in the North Atlantic: 1990s–2000s

Feili Li, Young-Heon Jo, W. Timothy Liu, Xiao-Hai Yan

First Published: 3 August 2012 Vol: 39, L15604 | DOI: 10.1029/2012GL052556

KEY POINTS

- A dipole pattern appears in the SSHA trends and low frequency SSHA oscillations
- The SSHA in the North Atlantic asymmetrically respond to the NAO forcing
- A reversal of the SSHA trend might relate to the propagation of AMOC variations

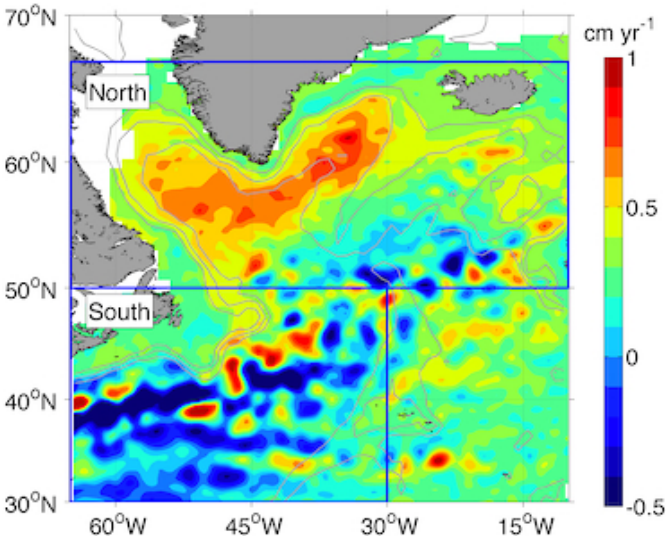

1 of 4

Influence of the Pacific Decadal Oscillation on phytoplankton phenology and community structure in the western North Pacific

Sanae Chiba, Sonia Batten, Kosei Sasaoka, Yoshikazu Sasai, Hiroya Sugisaki
First Published: 2 August 2012 Vol: 39, L15603 | DOI: 10.1029/2012GL052912

KEY POINTS

- PDO influences phytoplankton seasonality and community structure
- Variation of seasonal ML processes are crucial for phytoplankton ecology

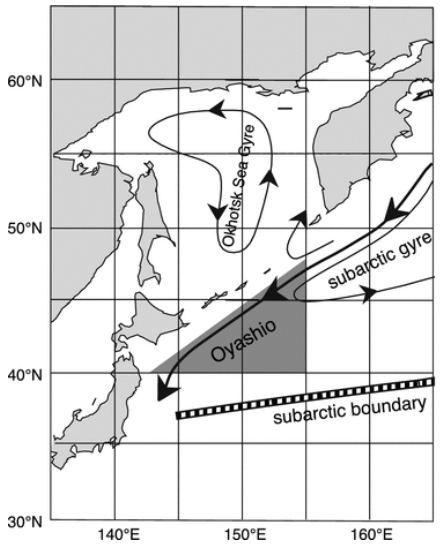

1 of 3

Observations of the structure of turbulent mixing across the Kuroshio

Hitoshi Kaneko, Ichiro Yasuda, Kosei Komatsu, Sachihiko Itoh
First Published: 2 August 2012 Vol: 39, L15602 | DOI: 10.1029/2012GL052419

KEY POINTS

- Quantification of turbulence level across the Kuroshio through composite mean
- Significantly elevated turbulence at the fronts especially on the cyclonic side
- Relationship between turbulence and geostrophic shear on the cyclonic side

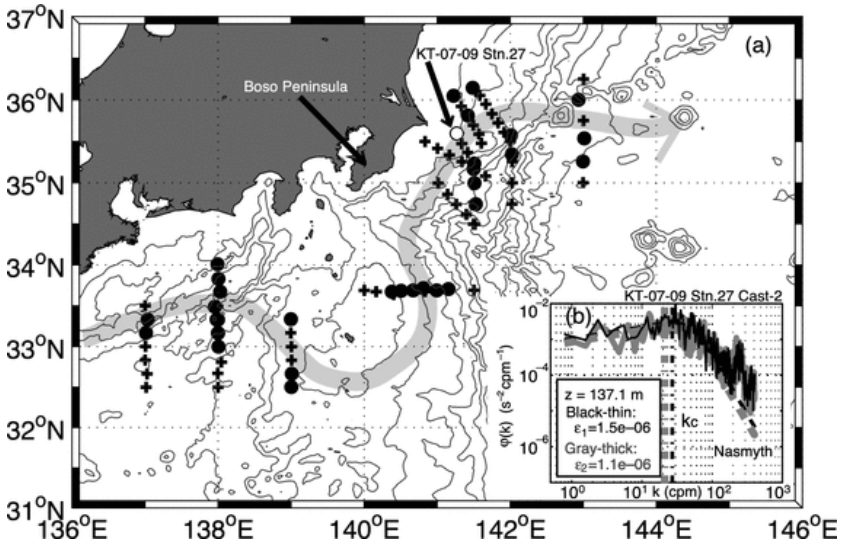

1 of 4

New constraints on European glacial freshwater releases to the North Atlantic Ocean

Frédérique Eynaud, Bruno Malaizé, Sébastien Zaragosi, Anne de Vernal, James Scourse, Claude Pujol, Elsa Cortijo, Francis E. Grousset, Aurélie Penaud, Samuel Toucanne, et al

First Published: 1 August 2012 Vol: 39, L15601 | DOI: 10.1029/2012GL052100

KEY POINTS

- Paleosalinity changes are documented in the Bay of Biscay for the last glacial
- Paleosalinity values derived from two independent methods converge
- Paleosalinity events accurately illustrate the sequencing of climate excursions

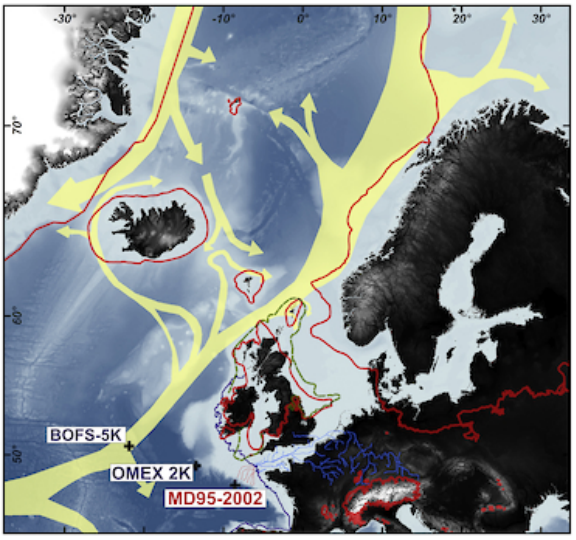

1 of 3

Planets

Can tidal tomography be used to unravel the long-wavelength structure of the lunar interior?

Shijie Zhong, Chuan Qin, Geruo A, John Wahr

First Published: 15 August 2012 Vol: 39, L15201 | DOI: 10.1029/2012GL052362

KEY POINTS

- A lunar mantle with laterally varying structure produces non-degree-2 response
- The non-degree-2 response may be extracted from satellite data
- The lateral variations in lunar structure help understand lunar mantle dynamics

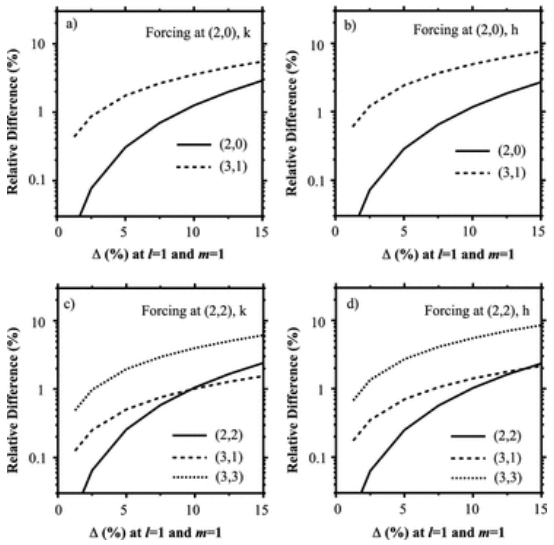

1 of 2

Solid Earth

Seasonal hydrological loading in southern Alaska observed by GPS and GRACE

Yuning Fu, Jeffrey T. Freymueller, Tim Jensen

First Published: 15 August 2012 Vol: 39, L15310 | DOI: 10.1029/2012GL052453

KEY POINTS

- GPS and GRACE observe highly correlated seasonal loading deformation
- The effects of atmosphere and non-tidal ocean loading are important
- GRACE models can correct seasonal displacements for campaign GPS

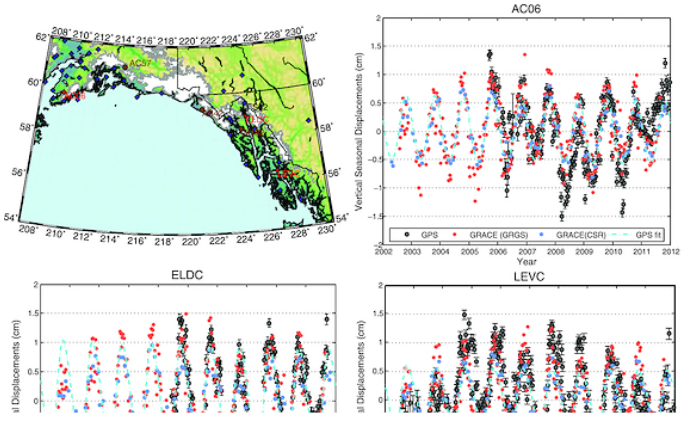

1 of 5

Beyond receiver functions: Passive source reverse time migration and inverse scattering of converted waves

Xuefeng Shang, Maarten V. de Hoop, Robert D. van der Hilst

First Published: 11 August 2012 Vol: 39, L15308 | DOI: 10.1029/2012GL052289

KEY POINTS

- A new seismic migration method exploiting denseseismic array data is proposed
- Full wave equation and inverse scattering theory are incorporated in the method
- Superior to traditional receiver function in complex geological environments

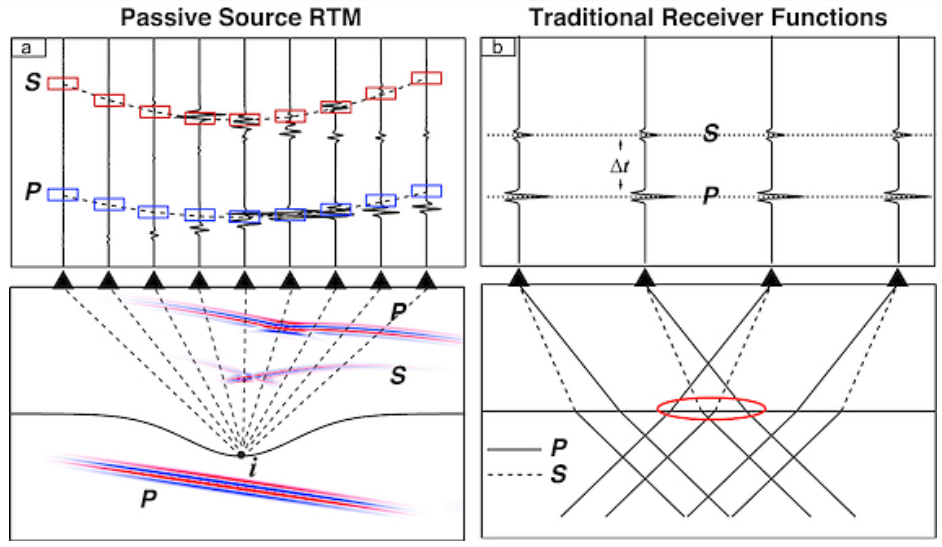

1 of 4

A slow slip event in the south central Alaska Subduction Zone and related seismicity anomaly

Meng Wei, Jeffrey J. McGuire, Eliza Richardson

First Published: 11 August 2012 Vol: 39, L15309 | DOI: 10.1029/2012GL052351

KEY POINTS

- We found a new slow slip event in the south central Alaska

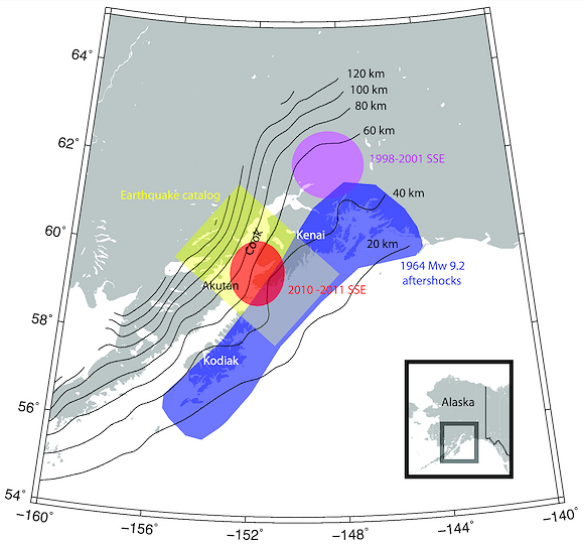

1 of 3

Volcanic edifice weakening via decarbonation: A self-limiting process?

Silvio Mollo, Michael J. Heap, Gianluca Iezzi, Kai-Uwe Hess, Piergiorgio Scarlato, Donald B. Dingwell

First Published: 10 August 2012 Vol: 39, L15307 | DOI: 10.1029/2012GL052613

KEY POINTS

- Deacarbonation reaction weakens sub-volcanic sedimentary basements
- If decarbonation is halted, rocks continue to degrade via thermal microcracking
- Sub-volcanic carbonate basements are at significant risk for instability

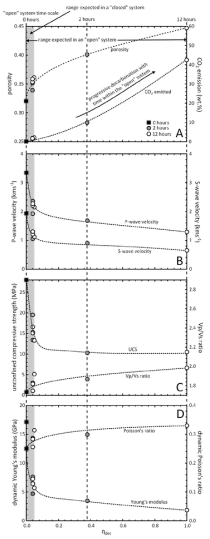

1 of 4

Sizing up the bubbles that produce very fine ash during explosive volcanic eruptions

Kimberly Genareau, Alexander A. Proussevitch, Adam J. Durant, Gopal Mulukutla, Dork L. Sahagian

First Published: 8 August 2012 Vol: 39, L15306 | DOI: 10.1029/2012GL052471

KEY POINTS

- Simple ash particles preserve the imprint of individual vesicles
- Stereo-SEM imaging allows quantification of original bubble volumes
- The measured bubbles burst during eruption to produce hazardous very fine ash

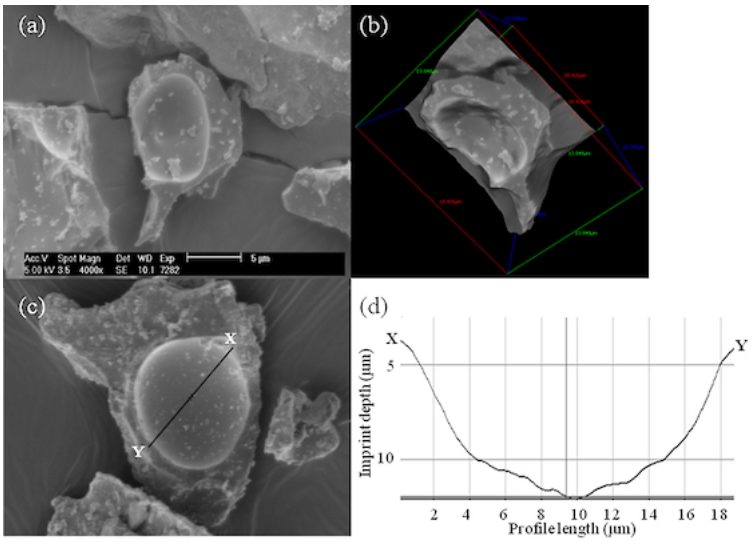

1 of 4

Equivalency of geologic and geodetic rates in contractional orogens: New insights from the Pamir Frontal Thrust

Tao Li, Jie Chen, Jessica A. Thompson, Douglas W. Burbank, Weipeng Xiao

First Published: 7 August 2012 Vol: 39, L15305 | DOI: 10.1029/2012GL051782

KEY POINTS

- At time scales of ~18 and 350 ka, Pamir Frontal Thrust shortening is ~6-7 mm/a
- Across this time range, geologic and geodetic rates appear equivalent on the PFT
- Such equivalency is likely dependent on fault geometry, mechanics and time scale

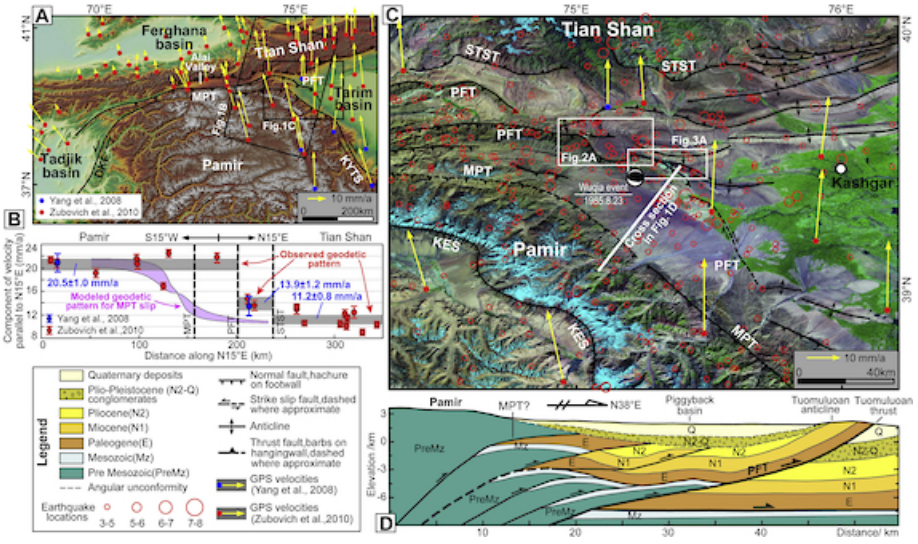

1 of 4

Heterogeneities along the 2009 L'Aquila normal fault inferred by the b-value distribution

Pasquale De Gori, Francesco Pio Lucente, Anna Maria Lombardi, Claudio Chiarabba, Caterina Montuori

First Published: 4 August 2012 Vol: 39, L15304 | DOI: 10.1029/2012GL052822

KEY POINTS

- Spatial variability of b-values on the L'Aquila fault plane
- Earthquake nucleates within the to low b-value area
- Largest slip occurs in normal-to-high b-values portion of the fault plane

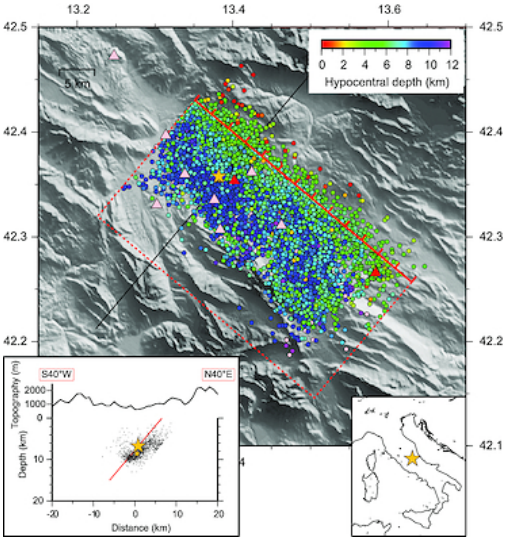

1 of 3

The 2012 Mw 8.6 Sumatra earthquake: Evidence of westward sequential seismic ruptures associated to the reactivation of a N-S ocean fabric

Claudio Satriano, Eszter Kiraly, Pascal Bernard, Jean-Pierre Vilotte

First Published: 3 August 2012 Vol: 39, L15302 | DOI: 10.1029/2012GL052387

KEY POINTS

- Source mechanism of the great strike-slip intraplate earthquake
- Sequential rupture: triggering, reactivation of seafloor fossil structures
- Backprojection avoiding biases by a-priori rupture parameterization

Highlight

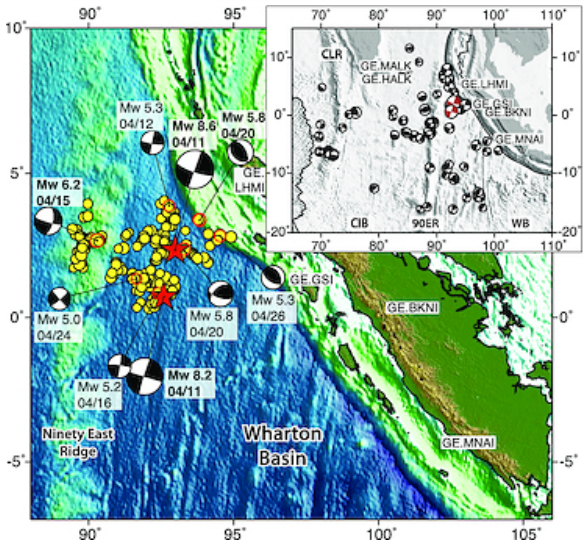

1 of 4

Progressive microscopic damage associated with fault growth

T. Tamarkin, A. Ougier-Simonin, Wenlu Zhu

First Published: 3 August 2012 Vol: 39, L15303 | DOI: 10.1029/2012GL052487

KEY POINTS

- A novel approach to stabilize fault growth and investigate failure process
- Brittle fracture emerges from coalescence of microscopic damage
- Grain crushing is associated with brittle faulting

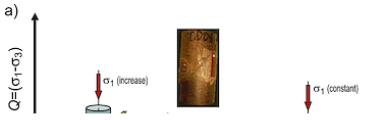

1 of 3

Regional extent of the large coseismic slip zone of the 2011 Mw 9.0 Tohoku-Oki earthquake delineated by on-fault aftershocks

Aitaro Kato, Toshihiro Igarashi

First Published: 2 August 2012 Vol: 39, L15301 | DOI: 10.1029/2012GL052220

KEY POINTS

- On-fault aftershocks enable us to outline the outer edge of the large-slip zone
- The outer edge of the large-slip zone shows a remarkably complex shape
- Stress increase by abrupt termination of the large-slip triggers an afterslip

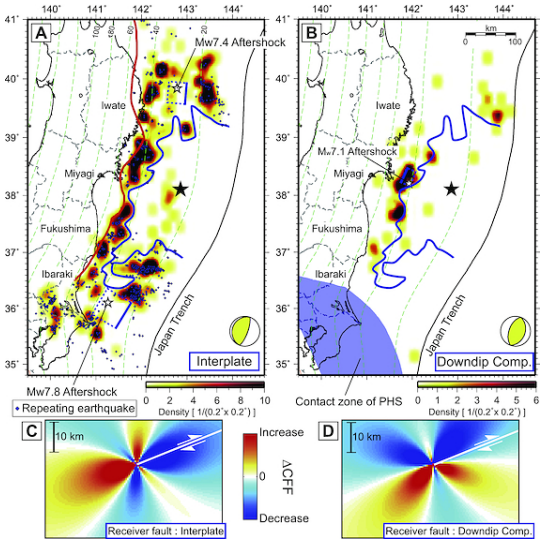

1 of 3

Space Sciences

Asymmetric magnetosphere deformation driven by hot flow anomaly(ies)

J. Šafránková, O. Goncharov, Z. Němeček, L. Přech, D. G. Sibeck

First Published: 15 August 2012 Vol: 39, L15107 | DOI: 10.1029/2012GL052636

KEY POINTS

- Interaction of the IMF rotation with the bow shock
- Large deformation of magnetopause and bow shock surfaces
- Creation of a pair of HFAs at dawn and dusk

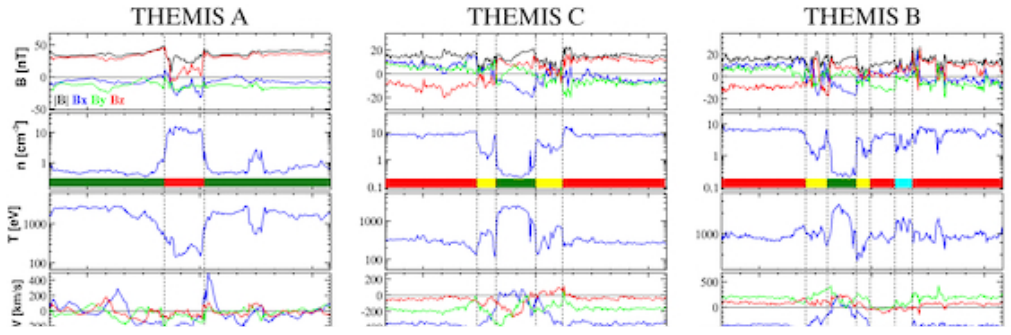

1 of 4

Reduction in field-aligned currents preceding and local to auroral substorm onset

Kyle R. Murphy, Ian R. Mann, I. Jonathan Rae, Colin L. Waters, Brian J. Anderson, David K. Milling, Howard J. Singer, Haje Korth

First Published: 9 August 2012 Vol: 39, L15106 | DOI: 10.1029/2012GL052798

KEY POINTS

- Localised reduction FACs is observed preceding and local to auroral onset
- Change in FACs is the result of a change in magnetosphere-ionosphere coupling
- These observations have important implications in any substorm paradigm

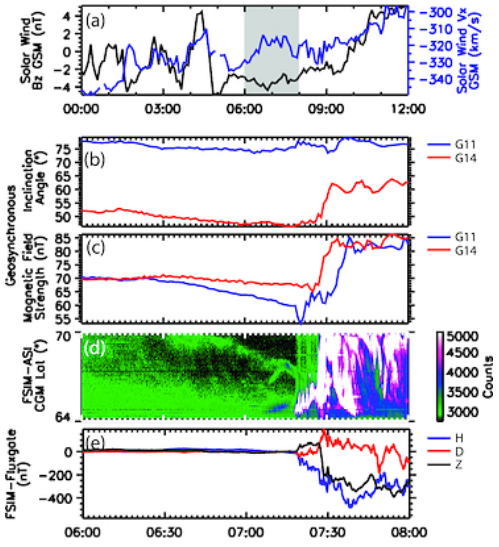

1 of 4

Necessity of substorm expansions in the initiation of steady magnetospheric convection

J. Kissinger, R. L. McPherron, T.-S. Hsu, V. Angelopoulos, X. Chu

First Published: 8 August 2012 Vol: 39, L15105 | DOI: 10.1029/2012GL052599

KEY POINTS

- Clear AL substorms precede 92% of SMC events
- Only 1% of SMCs have no preceding substorm signatures
- After a substorm, magnetosphere stabilizes into SMC under continued IMF driving

Highlight

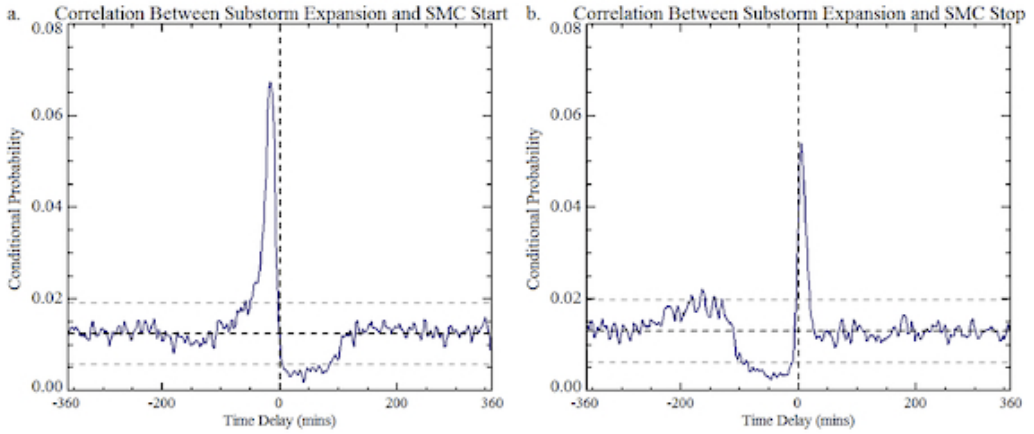

1 of 4

On the Edgeworth-Kuiper Belt dust flux to Saturn

Andrew R. Poppe, Mihály Horányi

First Published: 8 August 2012 Vol: 39, L15104 | DOI: 10.1029/2012GL052530

KEY POINTS

- We calculate the Edgeworth-Kuiper Belt dust flux to Saturn
- This model is based on New Horizons Student Dust Counter and Pioneer 10 data
- Flux of EKB dust to Saturn is significantly different from previous estimates

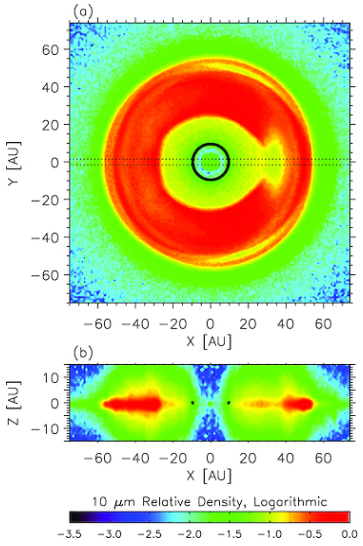

1 of 3

Peak emission altitude of Saturn's H_3^+ aurora

Tom S. Stallard, Henrik Melin, Steve Miller, Sarah V. Badman, Robert H. Brown, Kevin H. Baines

First Published: 7 August 2012 Vol: 39, L15103 | DOI: 10.1029/2012GL052806

KEY POINTS

- The peak H3+ emission altitude is at ~1150 km, intrinsically useful information
- This is very similar to the UV peak, suggesting the same precipitation source
- Higher altitude emission is weaker than past observations or modelling suggested

1 of 2

Parameterized lifetime of radiation belt electrons interacting with lower-band and upper-band oblique chorus waves

Xudong Gu, Yuri Y. Shprits, Binbin Ni

First Published: 2 August 2012 Vol: 39, L15102 | DOI: 10.1029/2012GL052519

KEY POINTS

- The lifetimes are dependent on energy, L shell and Kp index
- The accuracy of parameterization is less than 50%
- Valuable for simulations of radiation belt and ring current electrons

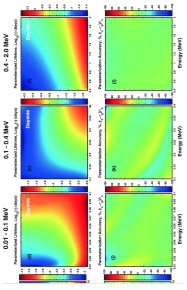

1 of 2

Equatorially confined warm trapped ions at around 100 eV near the plasmapause

M. Yamauchi, I. Dandouras, H. Rème, F. El-Lemdani Mazouz

First Published: 1 August 2012 Vol: 39, L15101 | DOI: 10.1029/2012GL052366

KEY POINTS

- Ring distribution for He+ rather than pancake distribution
- Variable ratio of characteristic energies between He+ and H+
- Time scale of development of about one hour

Open Access

1 of 4

The Cryosphere

Minimum distribution of subsea ice-bearing permafrost on the U.S. Beaufort Sea continental shelf

Laura L. Brothers, Patrick E. Hart, Carolyn D. Ruppel

First Published: 7 August 2012 Vol: 39, L15501 | DOI: 10.1029/2012GL052222

KEY POINTS

- First regional map of subsea permafrost on the US Beaufort continental shelf
- Permafrost layer refractions do not extend beyond 30 km of shore
- Assumptions about this shelf's offshore extent of permafrost should be revised

1 of 2

Current Issue

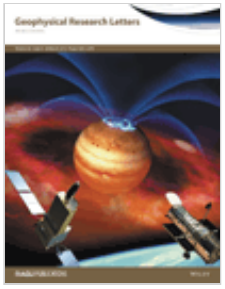

Volume 42
Issue 6
28 March 2015

All Issues
Browse a free sample issue

Find an article

and

or

Stay Connected to Eos

Access Eos Archive Issues

Issues from 1997-2014 are freely available to the public.

Older issues are available through AGU membership or through an institutional subscription.

Journal Resources

Call for Papers

Special Section Proposal Form

Personal Choice

Terms of Use

Cover Gallery

Institutional Subscription Rates

Get RSS Feed

Featured Special Collection

The Early Results from the Van Allen Probes

NASA's Van Allen Probes mission is designed to acquire data to solve key questions about the energetics and dynamics of the Earth's Van Allen Radiation belts that have arisen from active research in the domain in the past decades.

Editors' Highlights

- **What Causes Sunspot Pairs?**
- **Water Beneath the Surface of Mars, Bound up in Sulfates**
- **When Predicting Drought Risk, Do Not Overlook Temperature**
- **Changing Patterns in U.S. Air Quality**

See all »

Download the app

Download the Geophysical Research Letters app on your iPad

Upcoming AGU Meetings

Triennial Earth-Sun Summit

26 Apr - 1 May 2015
Indianapolis, Indiana, USA

2015 Joint Assembly

3-7 May 2015
Montreal, Canada

Chapman Conference on Evolution of the Asian Monsoon and its Impact on Landscape, Environment and Society: Using the Past as the Key to the Future

14-19 June 2015
Hong Kong SAR, China

See all »